Tracking adaptive optics scanning laser ophthalmoscope

R. Daniel Ferguson[*a], Daniel X. Hammer[a], Chad E. Bigelow[a], Nicusor V. Iftimia[a], Teoman E. Ustun[a], Stephen A. Burns[b], Ann E. Elsner[b], David R. Williams[c]

[a]Physical Sciences Inc., 20 New England Business Center, Andover MA 01810;
[b]Indiana University School of Optometry, Bloomington IN 47405;
[c]Center for Visual Science, University of Rochester, Rochester NY 14627

ABSTRACT

Active image stabilization for an adaptive optics scanning laser ophthalmoscope (AOSLO) was developed and tested in human subjects. The tracking device, a high speed, closed-loop optical servo which uses retinal features as tracking target, is separate from AOSLO optical path. The tracking system and AOSLO beams are combined via a dichroic beam splitter in front of the eye. The primary tracking system galvanometer mirrors follow the motion of the eye. The AOSLO raster is stabilized by a secondary set of galvanometer mirrors in the AOSLO optical train which are "slaved" to the primary mirrors with fixed scaling factors to match the angular gains of the optical systems. The AO system (at 830 nm) uses a MEMS-based deformable mirror (Boston Micromachines Inc.) for wave-front correction. The third generation retinal tracking system achieves a bandwidth of greater than 1 kHz allowing acquisition of stabilized AO images with an accuracy of <10 μm. However, such high tracking bandwidth, required for tracking saccades, results in finite tracking position noise which is evident in AOSLO images. By means of filtering algorithms, the AOSLO raster is made to follow the eye accurately with reduced tracking noise artifacts. The system design includes simultaneous presentation of non-AO, wide-field (~40 deg) live reference image captured with a line scanning laser ophthalmoscope (LSLO) typically operating from 900 to 940 nm. High-magnification (1-2 deg) AOSLO retinal scans easily positioned on the retina in a drag-and-drop manner. Normal adult human volunteers were tested to optimize the tracking instrumentation and to characterize AOSLO imaging performance. Automatic blink detection and tracking re-lock, enabling reacquisition without operator intervention, were also tested. The tracking-enhanced AOSLO may become a useful tool for eye research and for early detection and treatment of retinal diseases.

Keywords: Adaptive optics, scanning laser opthalmoscopy, retinal tracking

1. INTRODUCTION

The recent introduction of adaptive optics scanning laser ophthalmoscopy (AOSLO)[1-4] for enhanced retinal imaging has opened new avenues of inquiry in visual science, and new therapeutic possibilities. AO correction provides near diffraction-limited optical access for SLO imaging with > 6 mm pupils, and significant benefits for precise, depth-controlled therapeutic beam or retinal stimuli placement. These methods may soon prove their worth in clinical applications, as well as eye research.

The benefits of AO will be widely applicable from the standpoint of ordinary corneal and lenticular aberrations. However, there are numerous clinical issues encountered in the patient population which may limit the utility of AO. Reduced clarity of optical media in elderly patients, and the ability of low vision subjects to fixate and minimize head motion, will tend to reduce contrast, image stability and the fraction of useable frames obtained in an imaging session. Such limitations may or may not be addressable with image post-processing over low-contrast tracts of moving retina. And precision laser targeting in real time would not benefit from this in any case.

At the very high magnifications (~1 deg FOV) associated with AO imaging of cones, local pathologies or lesions, micro-circulation anomalies, feeder vessels, etc., the effects of eye motion across frames are effectively amplified. Net

[*] ferguson@psicorp.com; phone 1 978 689-0003; fax 1 978 689-3232; http://www.psicorp.com

motion may be < 0.5 deg for very good fixators, but this is already half of the frame dimension. Furthermore, with few landmarks, precise knowledge of where the AO raster is on the retina at any given moment is often lacking. Image distortion, drift and saccades with compromised fixation may make AOSLO imaging quite difficult in clinical practice. For these reasons, we have combined AOSLO imaging with auxiliary tracking and imaging capabilities which are readily integrated into AOSLO systems with minimal impact on the primary imaging function. Designs which offer additional benefits for normal AO operation are described.

2. MATERIALS AND METHODS

The tracking adaptive optics scanning laser ophthalmoscope (TAOSLO) system combines high-magnification scanning laser ophthalmoscopy (SLO), adaptive optics (AO), wide-field line-scanning imaging and retinal tracking. High bandwidth closed-loop optical retinal tracking mitigates the effects of eye motion and provides reproducible retinal coordinates for efficient collection of back-scattered light or delivery of focused beams. A simplified block diagram of the TAOSLO is shown in Figure 1. A detailed discussion of the human and animal experiments, and TAOSLO performance can be found in another paper in this proceedings.[5] The system uses a dual-imaging approach that simultaneously displays confocal wide-field and high magnification retinal views from the front end TSLO and AOSLO sub-systems, respectively. Thus the position of the AOSLO raster, which often cannot be unambiguously determined from the retinal image information within such a small field, is precisely known, displayed, and controlled by the user. The AO system includes Hartmann-Shack wave-front sensor and deformable mirror wave-front compensator. Diffraction-limited beams are delivered to the eye via a port placed behind the deformable mirror.

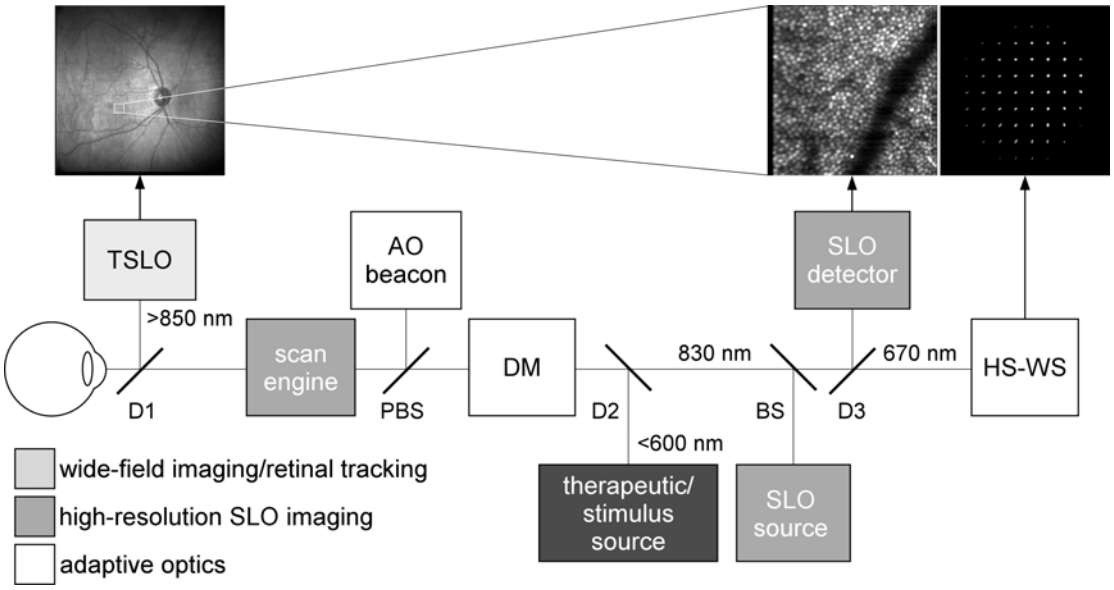

Figure 1: Simplified block diagram of TAOSLO system. DM: deformable mirror, HS-WS: Hartmann-Shack wavefront sensor, Dx: dichroic beamsplitter, PBS: pellicle beamsplitter. Tracking SLO (TSLO) is an independent unit on the front of the instrument.

2.1 TSLO retinal tracking and imaging

The operation of the retinal tracking system has been previously described.[6-9] Briefly, it is a closed-loop optical tracker that directly senses the movement of retinal features with a low-power confocal reflectometer beam (<250 μwatts at 1060 nm). The optic nerve head (with a bright reflection from the lamina cribrosa) is our primary tracking feature and the macular region is our primary imaging target. Galvanometer mirrors are steered to compensate eye rotation with a closed loop bandwidth of ~1 KHz. A wide-field line scanning laser opthalmoscope (LSLO)[10] and the tracking systems are combined in an independent unit (designated TSLO in Figure 1 above), and performs the tracking and wide-field imaging functions at the front end of the TAOSLO. The TSLO monitors eye motion with full tracking bandwidth and stabilizes the LSLO image.

The TSLO constitutes the "master" control loop: *x-y* error signals generated from the tracking beam confocal reflectometer are processed by a DSP controller to drive the x-y tracking mirror positions in real time. The TSLO requires wide-field optical access to the retina which is accomplished with a scan lens (85 mm) and a 30D ophthalmoscopic lens. This lens pair is not directly compatible with AOSLO imaging requirements. The TSLO and TAOSLO optical paths are instead combined at the pupil via a dichroic beamsplitter placed just in front of the eye. This is illustrated schematically in more detail in the unfolded TAOSLO optical layout in Figure 2 below.

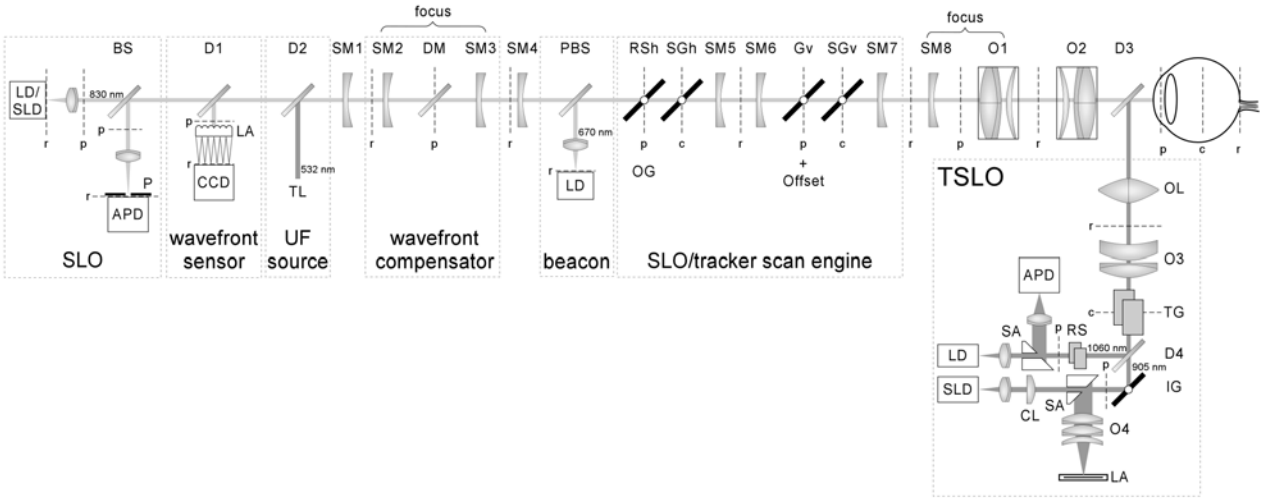

Figure 2: Unfolded optical layout of TAOSLO system.

The AOSLO layout itself is rather conventional, with a series of pupil conjugates relayed though spherical mirror pairs, from the eye to the vertical scanner, the horizontal resonant scanner, the deformable mirror, the wavefront sensor, and the SLO detector. Because the AOSLO raster cannot pass through TSLO optics where the tracking loop is closed, two additional galvanometers (SGh and SGv) slaved to the TSLO tracking galvanometers are placed at appropriate conjugates within the path of the adaptive optics scanning laser ophthalmoscope. The inputs to the "slave" galvos in the TAOSLO are the scaled x-y position signals from the master galvanometers. This configuration requires a one-time calibration between master and slave galvanometers. By moving a fixation light, causing the eye to move to fixed locations, these scale factors are tuned so that the TAOSLO image appears fixed throughout. The TAOSLO thus moves precisely with the eye.

The slave tracking mirrors (SGh and SGv) are placed at conjugates to the center of rotation (c) of the eye. Because the mirrors pivot about the center of rotation of the eye while tracking, this produces simultaneous tracking of the pupil and retina during rotational eye motion we call line-of-sight tracking. This has the benefit of not altering the required AO correction during or after saccadic motion because the pupil is fixed. However, pupil motion due to head translation is not compensated. In order to address translation of the pupil, an additional pupil sensor is required. Presently, the wavefront sensor camera itself will be evaluated for this purpose and another nested control loop will be implemented to track a limited range of head motion. This may have significant benefit for clinical applications where bite-bar head stabilization is undesirable. The above master-slave tracking configuration has minimal impact on the AOSLO optical train. In addition to head motion tracking, design advantages include advanced slave position-signal filtering (see the discussion in Section 3.2)

In the current system configuration, all tracking functions are performed by a single set of stacked electronics boards. Communication between the tracking boards and host computer is through a USB 2.0 interface. Control parameters and reflectance, position, and error signals are passes to and from the tracking boards. The blink detection and track re-lock algorithms are similar to previous systems.[11] The control and processing electronics include a field programmable gated array (FPGA) chip that performs digital lock-in amplification and other pre-processing steps, a digital signal processor (DSP) that performs two proportional-integral-derivative (PID) control loops (for master and slave systems), and

analog-to-digital and digital-to-analog converters (ADC and DACs) to receive reflectometer signals and drive galvanometers. The DSP has a loop rate of 62.5 kHz (compared to 16 KHz in the previously-used real-time processing board) for a closed loop bandwidth > 1 kHz.[6] The tracking beam wavelength was moved to 1060 nm to accommodate typical superluminescent diodes (SLD) used in AOSLO and optical coherence tomography (OCT) systems.

2.2 TAOSLO opto-mechanical system

Key portions of the TAOSLO opto-mechanical system configuration is shown if Figure 3. The flying-spot raster uses a 12-kHz resonant scanner in the fast *x*-axis and a galvanometer in the slow *y*-axis. The entire resonant scanner is attached to a large, lower-speed galvanometer (Cambridge Technologies 6230). In such a configuration, offsets can be applied to both axes to track the pupil or create AOSLO montages. A near-infrared source (830-nm LD or 800-nm SLD with 30-nm bandwidth, Exalos Inc.) is used for SLO illumination and an avalanche photodiode detector (Hamamatsu Inc.) with confocal pinhole (100 and 200-µm diameter) is used for detection. The AO system uses a Hartmann-Shack wave-front sensor (HS-WS) comprised of a 65×65-element lenslet array (0.4-mm pitch and 25-mm focal length, Adaptive Optics Associates Inc.) and a 1024×1024-pixel CCD camera with a maximum frame rate of 60 Hz and camera-link interface (Dalsa Inc.). Wavefront sensing is done with a 670-nm AO beacon. The beacon is placed in front of the deformable mirror (DM) to minimize distortion from mirror surface irregularities and to de-couple mirror-induced wavefront errors during mirror-sensor calibration. It is placed behind the scanning mirrors to provide smoother spots and improve the accuracy of the centroid algorithm.[12] A 141-element MEMS-based DM (Boston Micromachines Inc.) is used for wave-front correction. The DM has a diameter of only 4.8-mm so long paths are not required to magnify the pupil.

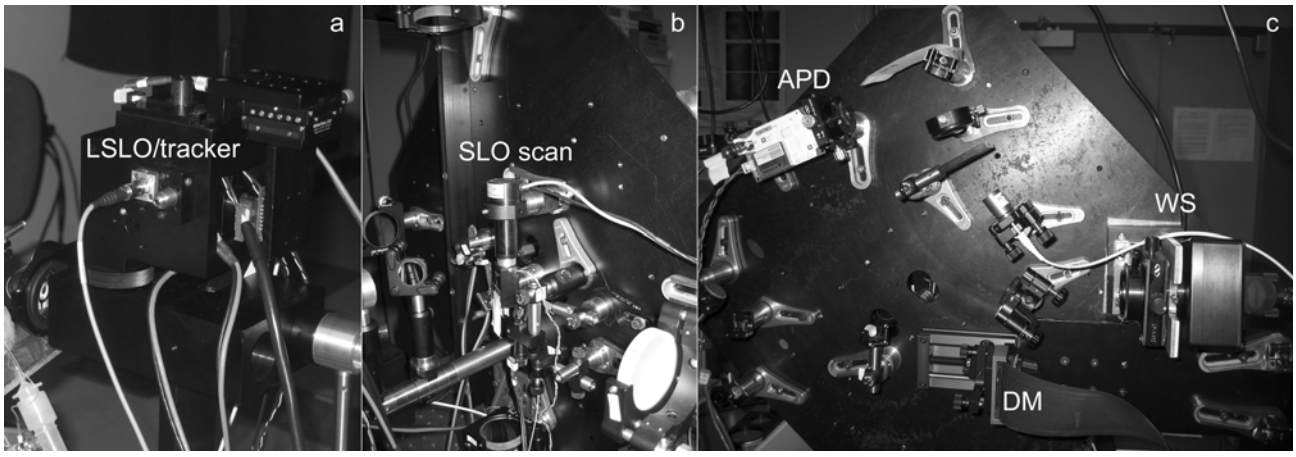

Figure 3: Photographs of (a) retinal tracking head, (b) AOSLO front plate, and (c) AOSLO back plate.

The optics de-magnify a 6-mm pupil through the small resonant scanner mirror, to fill the DM (to use all actuators) and magnify again to nearly fill the WS camera. A novel three-dimensional optical arrangement uses spherical mirrors to eliminate back-reflections, chromatic distortion, and dispersive pulse broadening for ultra-fast laser pulses, as well as minimize off-axis astigmatism. AOSLO focus adjust range is up to 10 diopters. TSLO focus is adjusted independently of the AOSLO focus. The AOSLO optical design achieves an error of <0.5 waves (at 800 nm) over ±6 deg on the retina including a front lens relay.

The LSLO source for wide-field imaging is a 905-nm SLD. The combined power of the four wavelengths that enter the eye – 670, 830, 905, and 1060-nm for the AO beacon, SLO beam, LSLO beam, and tracking beam – always remained below ANSI standard thresholds. Typical powers used were 35, 300, 200, and 100 µW, respectively.

2.3 Electronics and instrumentation

TAOSLO instrumentation is shown schematically in Figure 4 below. This is described in a bit more detail in the other proceedings paper.[5] The system includes 3 framegrabbers (analog for SLO, digital camera-link for WS, and digital for LSLO), a non-linear pixel clock to the analog SLO framegrabber to automatically linearize the sinusoidal scan produced

by the resonant scanner, digital timing boards to control the DM, and a 8×8 LED array for fixation controlled via the serial port. The pixel clock board provides vertical and horizontal synch signals to the framegrabber, and to the WS camera-link frame-grabber to avoid frame aliasing artifacts in the spots, and to the SLO SLD source for modulation and blanking. A fixed physical mask cannot be used in the optical system for a blanking region while the retinal tracker operates because the AOSLO raster moves as the eye moves. The LSLO and SLO systems do not need to be synchronized since they use optical paths entirely independent of one another. The LSLO camera acquires a 512×512-pixel frame at 15 frames/sec. The 12-kHz resonant frequency of the SLO scanner enables a 512×512-pixel frame rate up to ~25 frames/sec. In addition to acquisition and display of the three images, the software controls communication with the tracking board, WS spot position and slope calculation, AO (WS/DM) calibration, AO closed-loop operation, wave aberration and Zernicke coefficient calculation and display, and logging of tracking signals, AVI videos (from all three cameras), and single images in a variety of formats. When a live video was streamed to disk, two additional files were saved that contained track data (reflectance, *x*-*y* track mirror positions, and either the *x*-*y* error signals or the *x*-*y* slave mirror positions) in binary format and a text file that contained all system parameters and calibration factors.

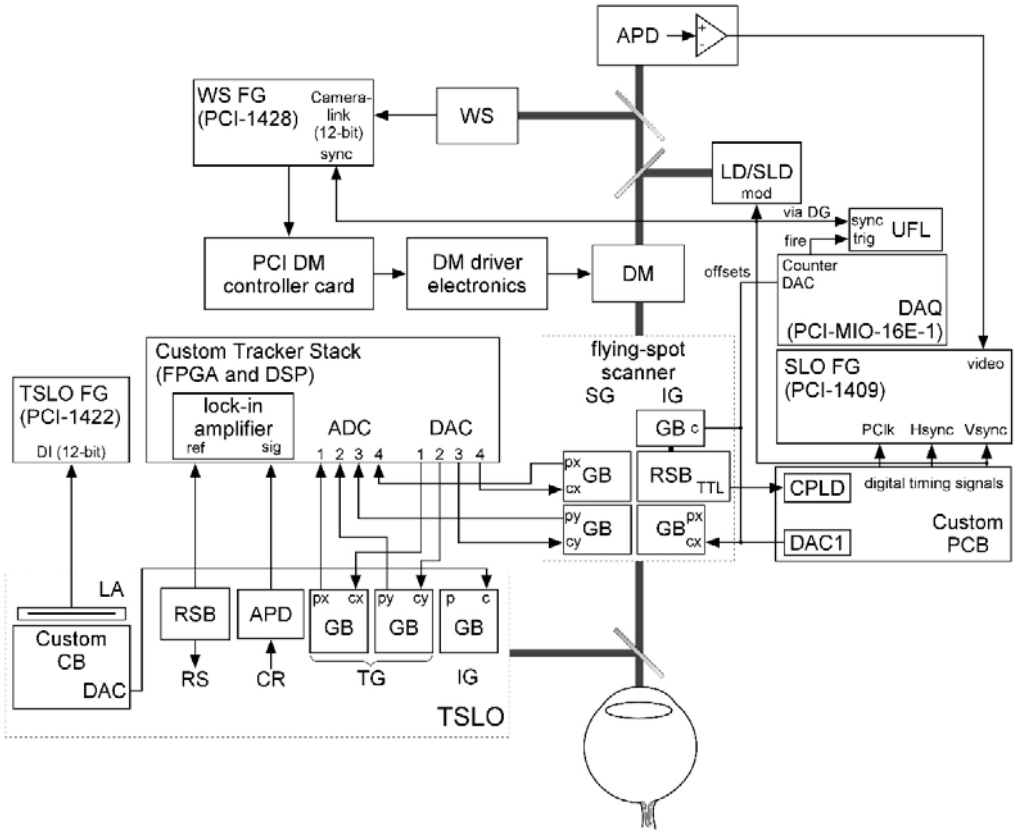

Figure 4: Instrumentation and electronics for the TAOSLO system.

The software GUI interface panels in LabVIEW (NI) are shown in Figure 5. The user can toggle between fundus and pupil views. The left panel, left side, shoes the live TSLO image. Overlays indicated the position of the tracking beam, the fixation light and the AOSLO raster (the AOSLO raster can usually be seen directly on the LSLO image). Left panel, right side shows the live AOSLO image. Tracking and imaging control pull-down tabs, and position, reflectance and error signal displays are seen below. The right panel displays live WS camera spots and computed slopes, and on the far right, DM display, wavefront error map, and graphical Zernicke term display are available. All function are integrated into a single host PC.

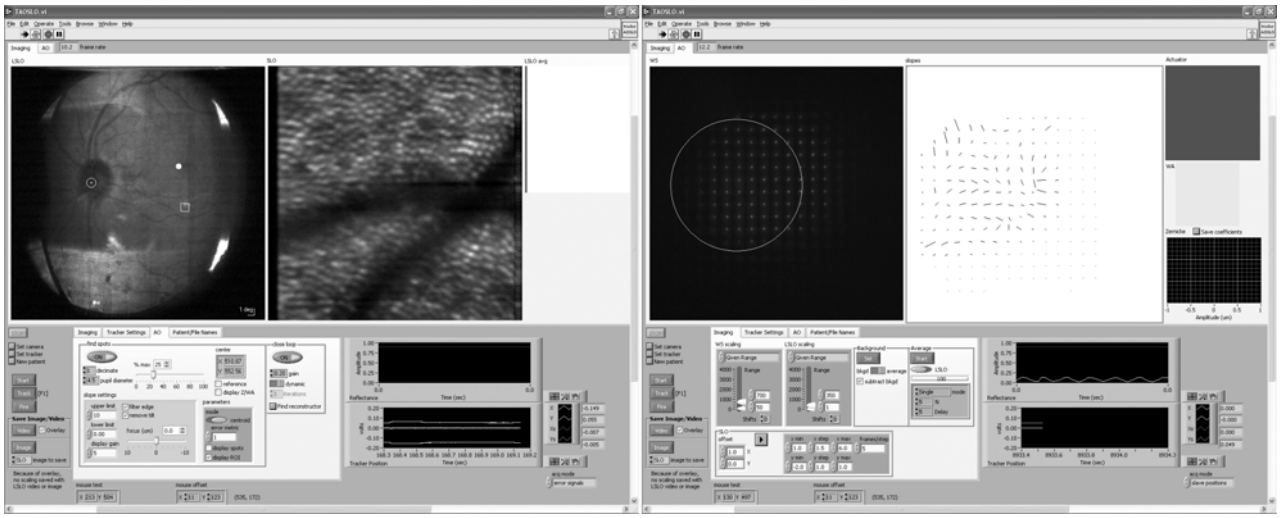

Figure 5: Graphical user interface of the TAOSLO system software. LSLO/SLO image tab (left panel) and WS image/calculated slopes tab (right panel).

3. RESULTS

3.1 Tracking performance of TAOSLO system

Human subjects were tested non-mydriatically (i.e., with 3-5-mm natural pupils). Even without dilation, we gained significant improvement in the SLO images with adaptive compensation of ocular aberrations. We were able to resolve the cone mosaic in all individuals (5 men, 1 woman, mean age = 36).

The tracking system was successfully demonstrated in all of these subjects. Video sequences, typically > 10 sec duration were captured in a number of conditions for comparison of imaging modes. Typically, the sequence was a particular combination of AO on/off and track on/off, and an automated mosaic captured with both tracking and AO.

For good fixators using an ~2 deg fixation target (in a green LED array) we expected drift and micro-saccadic motion to be confined with that region. This was generally true except for one subject displaying rapid gaze-evoked nystagmus-like motions. The AOSLO raster was set to approximately 1 deg.

Figure 6 shows a typical result. This subject was tracked at the lamina cribrosa, and imaged within few degrees of the fovea. Figure 6a shows the non-tracking case of eye motion derived from videos by a manual cone-tracking method. This subject show drift and <0.5 deg micro-saccades within the fixation target. Figure 6b shows the same subjects with tracking during similar eye motions. Rapid saccadic motions are evident, along with a few blinks with re-lock transients. Some tracking noise due to finite error signal SNR is in evidence, but is difficult to distinguish from ocular motor noise and other errors without further analysis. The resulting stabilized videos can be analyzed with the same manual cone tracking methods to find the residual errors. The resulting residual errors are plotted in Figure 6c.

The rms residual tracking error for this fixating subjects was 6 μm in both the x and y directions. No attempt was made to limit rms error by thresholding on tracking velocity or in the vicinity of blinks. This would improve the rms tracking performance, but even as it is, tracking performance is within a few cones.

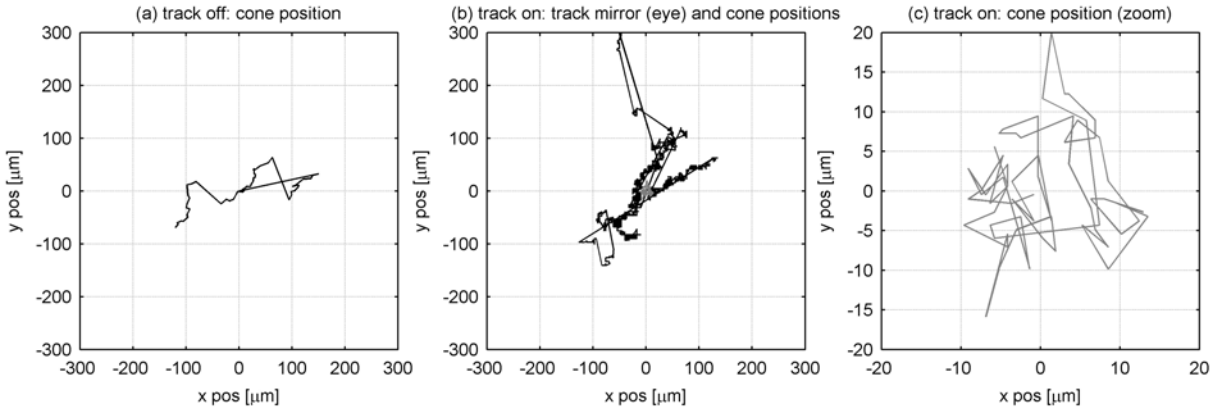

Figure 6: Cone and tracking mirror positions: (a) cone positions for a good fixator without tracking (three cones were followed and positions were corrected when switched between cones), (b) track mirror (i.e., eye, black line) and cone positions (gray line) for the same subject with tracking, (c) zoom of cone positions in (b) showing residual uncorrected motion.

3.2 Tracking errors and useable frames

The residual tracking errors are caused by several phenomena. The principal sources of tracking error are:

- Eye motion transients which occur because a finite error is needed to track rapid eye motion
- Geometric errors and distortion due to TSLO optics or eye cyclo-rotation (such errors scale with the distance between the tracked and imaged points)
- Finite error signal SNR at full tracking bandwidth which results in position jitter noise
- Fidelity, or lack of fidelity, of slave galvos in following the master tracking galvos
- Tracking perturbations from scattered or reflected light originating near the pupil.

A number of strategies to address these issues are being investigated in ongoing research and development to improve tracking precision and imaging data yield. For example, by thresholding video data on the tracking velocity (saccade/no saccade), some frames can be rejected when transient tracking errors are known to be most severe. Geometric and cyclo-rotation errors can be addressed by using tracking features closer to the image AOSLO field, or eventually with real-time/post LSLO image processing corrections. Position signal error noise and jitter, as well as slave fidelity can be addressed together with appropriate filtering algorithms. It is clearly not necessary to employ the full tracking bandwidth during most of AOSLO imaging because the eye drifts only slowly. But to avoid frequent loss of lock, fast tracking is required for saccades. Adaptive algorithms are being developed to yield the greatest fraction of useable, distortion-free TAOSLO frame area per imaging session. Pupil shift-related distortions and perturbations will be substantially eliminated with full pupil tracking. Finally, all of the available tracking signals can be used deterministically in post-processing to rapidly produce registration precision to less that one cone diameter.

In another test of the general utility of tracking for the AOSLO, subjects were instructed to move their gaze fixation point systematically around a 3 deg target roughly from 3 to 6 to 9 to 12 o'clock. This was intended to gauge the ability of the tracking system to maintain the same AOSLO field of view over larger motion ranges in a simulation of poor clinical fixation. The metric of quality was frame overlap area during a video record, with and without tracking.

Figure 7 shows the recorded tracking signals with tracking on during the first 12 seconds, and off for the last 12 seconds. The top trace shows reflectance vs. time. Note that while tracking, the reflectance is highly stable, since the tracking beam is fixed in one location. The second set of traces are the x-y tracking signals, showing the extent of motion. The bottom traces are the error signals; very small transients are visible during saccades which is a measure of the finite error needed to track—generally a small fraction of the tracking beam diameter.

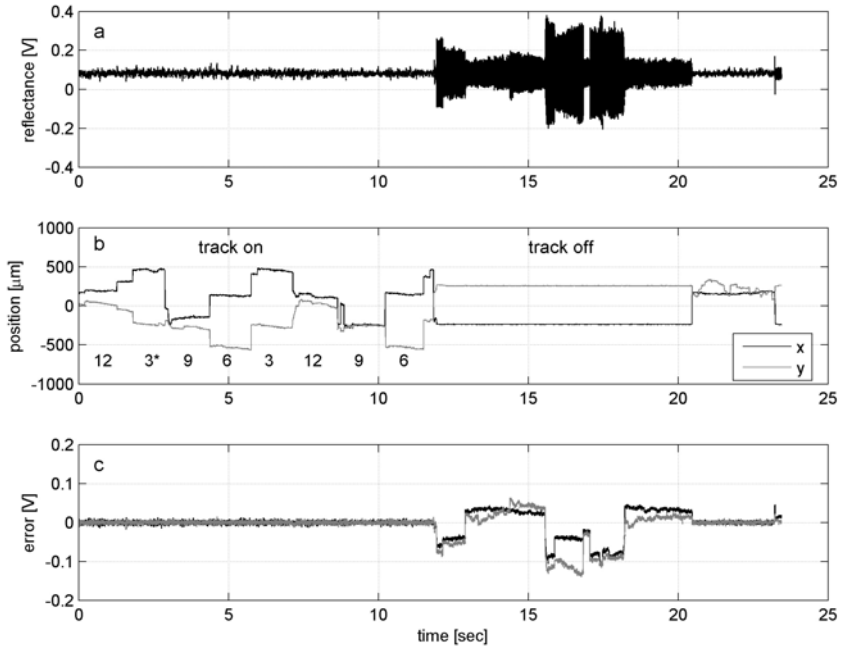

Figure 7: (a) Reflectance, (b) position, and (c) error signals for a subject looking sequentially at 4 positions (3, 6, 9, 12 o'clock) around the fixation light roughly 3-deg in diameter. (*Subject initially went clockwise 12-3 and then went counter-clockwise.)

Analysis of the resulting 1-deg TAOSLO video shows that the rms deviation during tracking is less 15µm or 5% of the frame dimension. The overlapping frame area is therefore ~90%. Without tracking, the frame overlap area is less than 10%. With adequate fixation, such as in the case above in Figure 6, frame overlaps of >50% are more typical.

4. DISCUSSION

The tracking adaptive optics scanning laser ophthalmoscope (TAOSLO) uses a novel optical system, integrated software platform, and advanced electronics and instrumentation for high resolution, aberration-corrected, stabilized dual-field imaging of the retina. The retinal tracking system uses a master-slave configuration and new enhancement strategies will push precision to the level of a single cone. Even for the best fixators, without retinal tracking eye motion can slew the field of regard to non-overlapping retinal locations reducing useable frames and image correspondence for longer duration scans and longitudinal studies. In a clinical scenario that includes predominantly elderly patients with limited ability to fixate, retinal tracking may prove invaluable for small AO fields. We demonstrated a significant improvement in the visualization of the retina with retinal tracking in all subjects tested to date.

ACKNOWLEDGEMENTS

This work was funded by NIH grant #1R21EB00311, and was performed, in part, in collaboration with the Center for Visual Science at the University of Rochester. We thank Rob Webb and Austin Roorda for helpful discussions.

REFERENCES

1. J. Liang, D. R. Williams, and D. Miller, "Supernormal vision and high-resolution retinal imaging through adaptive optics," J. Opt. Soc. Am. A **14**, 2884-2892 (1997).
2. A. Roorda and D. R. Williams, "The arrangement of the three cone classes in the living human eye," Nature, **397**, 520-522, 1999.

3. A. Roorda, F. Romero-Borja, W. J. Donnelly III, H. Queener, T. J. Hebert, and M. C. W. Campbell, "Adaptive optics scanning laser ophthalmoscopy," Opt. Express, **10**, 405-412, 2002.
4. Heidi Hofer, Joseph Carroll, Jay Neitz, Maureen Neitz, and David R. Williams, "Organization of the Human Trichromatic Cone Mosaic," J. Neuroscience, **25**, 9669-9679, 2005.
5. D. X. Hammer, R. D. Ferguson , C. E. Bigelow , N. V. Iftimia , T. E. Ustun , G. D. Noojin, D. J. Stolarski, H. M. Hodnett, M. L. Imholte, S. S. Kumru, M. N. McCall, C. A. Toth, B. A. Rockwell, "Precision targeting with a tracking adaptive optics scanning laser ophthalmoscope," Paper 6138-37, in Ophthalmic Technologies XVI, Eds: Manns, Soderberg, and Ho. (2006).
6. D. X. Hammer, R. D. Ferguson, J. C. Magill, M. A. White, A. E. Elsner, and R. H. Webb, "Image stabilization for scanning laser ophthalmoscopy," Opt. Express, **10,** 1542-1549, 2002, http://www.opticsexpress.org/abstract.cfm?URI=OPEX-10-26-1542.
7. D. X. Hammer, R. D. Ferguson, J. C. Magill, M. A. White, A. E. Elsner, and R. H. Webb, "Compact scanning laser ophthalmoscope with high speed retinal tracker," Appl. Opt., **42**, 4621-4632, 2003.
8. R. D. Ferguson, D. X. Hammer, L. A. Paunescu, S. Beaton, and J. S. Schuman, "Tracking Optical Coherence Tomography," Opt. Lett., **29**, 2139-2141, 2004.
9. D. X. Hammer, R. D. Ferguson, J. C. Magill, L. A. Paunescu, S. Beaton, H. Ishikawa, G. Wollstein, and J. S. Schuman, "An Active Retinal Tracker for Clinical Optical Coherence Tomography Systems," J. Biomed. Opt., **10**, 024038, 2005.
10. D. X. Hammer, R. D. Ferguson, T. E. Ustun, C. E. Bigelow, N. V. Iftimia, R. H. Webb, "Line-scanning laser ophthalmoscope," J. Biomed. Opt. (Special Issue for A. J. Welch), in press.
11. D. X. Hammer, R. D. Ferguson, N. V. Iftimia, T. E. Ustun, G. Wollstein, H. Ishikawa, M. L. Gabriele, W. D. Dilworth, L. Kagemann, and J. S. Schuman, "Advanced scanning methods with tracking optical coherence tomography," Opt. Express, **13**, 7937-7947, 2005. http://www.opticsexpress.org/abstract.cfm?URI=OPEX-13-20-7937.
12. H. Hofer, P. Artal, B. Singer, J. L. Aragón, and D. R. Williams, "Dynamics of the eye's wave aberration," J. Opt. Soc. Am. A., **18**, 497, 2001.